

# Edge detection and mathematic fitting for corneal surface with Matlab software

Yue Di<sup>1</sup>, Mei-Yan Li<sup>2</sup>, Tong Qiao<sup>1</sup>, Na Lu<sup>3</sup>

<sup>1</sup>Department of Ophthalmology, Shanghai Children's Hospital, Shanghai Jiaotong University, Shanghai 200062, China

<sup>2</sup>Department of Ophthalmology, Eye & ENT Hospital Fudan University, Fenyang Road 83, Shanghai 200031, China

<sup>3</sup>Department of Radiology, Huashan Hospital North, Fudan University, 108 Luxiang Road, Shanghai 201907, China

**Co-first authors:** Yue Di and Mei-Yan Li

**Correspondence to:** Tong Qiao. Department of Ophthalmology, Children's Hospital of Shanghai, Shanghai Jiaotong University, 355 Luding Road, Shanghai 200062, China. Qiaojoel@163.com; Na Lu. Department of Radiology, Huashan Hospital North, Fudan University, 108 Luxiang Road, Shanghai 201907, China. drluna@126.com

Received: 2016-03-17 Accepted: 2016-12-08

## Abstract

• **AIM:** To select the optimal edge detection methods to identify the corneal surface, and compare three fitting curve equations with Matlab software.

• **METHODS:** Fifteen subjects were recruited. The corneal images from optical coherence tomography (OCT) were imported into Matlab software. Five edge detection methods (Canny, Log, Prewitt, Roberts, Sobel) were used to identify the corneal surface. Then two manual identifying methods (ginput and getpts) were applied to identify the edge coordinates respectively. The differences among these methods were compared. Binomial curve ( $y=Ax^2+Bx+C$ ), Polynomial curve [ $p(x)=p_1x^n+p_2x^{n-1}+...+p_nx+p_{n+1}$ ] and Conic section ( $Ax^2+Bxy+Cy^2+Dx+Ey+F=0$ ) were used for curve fitting the corneal surface respectively. The relative merits among three fitting curves were analyzed. Finally, the eccentricity (e) obtained by corneal topography and conic section were compared with paired t-test.

• **RESULTS:** Five edge detection algorithms all had continuous coordinates which indicated the edge of the corneal surface. The ordinates of manual identifying were close to the inside of the actual edges. Binomial curve was greatly affected by tilt angle. Polynomial curve was lack of geometrical properties and unstable. Conic section could calculate the tilted symmetry axis, eccentricity, circle center, etc. There were no significant differences between 'e' values by corneal topography and conic section ( $t=0.9143$ ,  $P=0.3760 > 0.05$ ).

• **CONCLUSION:** It is feasible to simulate the corneal surface with mathematical curve with Matlab software. Edge detection has better repeatability and higher efficiency. The manual identifying approach is an indispensable complement for detection. Polynomial and conic section are both the alternative methods for corneal curve fitting. Conic curve was the optimal choice based on the specific geometrical properties.

• **KEYWORDS:** Matlab software; edge detection; curve fitting; mathematic simulation; optical coherence tomography; corneal topography

**DOI:10.18240/ijo.2017.03.02**

Di Y, Li MY, Qiao T, Lu N. Edge detection and mathematic fitting for corneal surface with Matlab software. *Int J Ophthalmol* 2017;10(3): 336-342

## INTRODUCTION

The precise explanation of visual signal requires the eye's power to focus incoming rays of light on the retina<sup>[1]</sup>. Lots of attempts have been tried to make the optical system of the human eye simpler<sup>[2-3]</sup>. The Gullstrand schematic eye is the model from which mathematical values for the eye's optical characteristics were derived<sup>[4]</sup>. The refraction index product of the medium of the incoming ray and the sine of the angle of incidence of the incident ray is equal to the product of the same terms of the refracted ray. The refracted ray is designated:  $n\sin I=n'\sin I'$  (Snell law)<sup>[5]</sup>. Analyzing optical systems by tracing rays based on Snell law is regarded as a common method in technical optics<sup>[5-6]</sup>. In the schematic eye, the cornea is assumed to be the only refracting surface. If we want to assess the effect on light rays as they pass through different media like cornea, the premise is to define the corneal surface accurately. Then, mathematics equation is applied to simulate the optical characteristic. Obviously it requires a lot of calculations including geometry, trigonometry, conic sections, and differential equations.

In this field, optical coherence tomography (OCT) systems are employed in various applications, especially in ophthalmology where it can be utilized to obtain detailed images including the cornea<sup>[7-8]</sup>. Meanwhile, Matlab (matrix laboratory) is a multi-

paradigm numerical computing environment and fourth-generation programming language<sup>[9-10]</sup>. Edge detection in Matlab has been widely applied, which is an image processing technique to extract useful structural information from different vision objects and dramatically reduce the amount of data to be processed<sup>[11-12]</sup>. Common edge detection includes ‘Sobel’, ‘Canny’, ‘Prewitt’, ‘Roberts’, and ‘Log’. In the ideal case, the result of applying an edge detector to an image may lead to a set of continuous curves that indicate the edges of objects. If the edge detection step is successful, the subsequent task of interpreting the information contents in the original image may therefore be substantially simplified. However, it is not always possible to obtain ideal edges from real images. In this case, ‘ginput’ and ‘getpts’ functions in Matlab raise crosshairs in the axes to identify points in the figure manually. Thus, in the current research, we identify the corneal surface with five edge detection algorithms, and compare the differences between edge detection and manual identifying methods.

Least square is a significant method of fitting a curve to data points so as to minimize the sum of the squares of the distances of the points from the curve<sup>[13]</sup>. Base on least square, curve fitting is the process of constructing a curve that has the best fit to a sequence of data points<sup>[14-15]</sup>. The fitted curves could be used as an aid for data visualization. Curve Fitting Tool in Matlab provides ‘polyfit’ function, which could find the coefficients of a polynomial  $p(x)$  of degree ‘n’ that fits the data, [Syntax:  $p(x)=p_1x^n+p_2x^{n-1}+\dots+p_nx+p_{n+1}$ ]<sup>[16-17]</sup>. If the degree n is 2, it is Binomial curve, namely, parabola. (syntax:  $y=Ax^2+Bx+C$ ). Meanwhile, as a circular curve, the corneal surface could be also regarded as conic section<sup>[18]</sup> [syntax:  $Ax^2+Bxy+Cy^2+Dx+Ey+F=0$ ]. Therefore, the relative merits were statistically analyzed among these three curve fitting equations.

In mathematics, eccentricity, denoted ‘e’, is a significant parameter associated with conic section<sup>[19]</sup>. It can be thought of a measure of how much the conic section deviates from being circular. (Circle:  $e=0$ ; ellipse:  $0<e<1$ ; parabola:  $e=1$ ; hyperbola:  $e>1$ ). Thus, in the current study, the ‘e’ values by corneal topography and conic section were compared further.

## SUBJECTS AND METHODS

**Corneal Surface Edge Detection** First, fifteen volunteers were recruited (8 males and 7 females, age 7-11 years old). Approval was obtained from the institutional review board of Fudan University (2015-05-01). Participants provided their written informed consent to participate in this study. All the left eyes were selected, the refractions, curvatures were collected. Afterwards, corneal images (resolution 868×380) from Fourier domain OCT (Optovue RTVue, MA, USA) were selected randomly and imported into Matlab R 2010b (Math

Works, MA, USA) software (horizontal direction scan). After using ‘imread’ and ‘imshow’ functions, these images were displayed in a two-dimensional graphics. (x-coordinate: 0-868; y-coordinate: 0-380, Figure 1A).

Edge detection methods: First, the originate images were transformed into binary images using ‘im2bw’ functions to sharpen the margin. Then, five edge detection algorithms include ‘Sobel’, ‘Canny’, ‘Prewitt’, ‘Roberts’, and ‘Log’ were applied to the images respectively (Figure 1B-1F). Afterward, non-target areas were removed, then the edge coordinates were acquired by ‘find’ functions<sup>[11]</sup>. In this way, five edge detection algorithms were compared in one graph.

Manual identifying methods: Matlab provides ‘ginput’ and ‘getpts’ functions to identify appointed points from the axes and returns their x- and y-coordinates in the x and y column vectors. In such two ways, we can position the cursor with the mouse to acquire the coordinates from corneal surface (Figure 1G, 1H).

**Corneal Surface Curve Fitting Methods** First, ‘polyfit (x, y, 2)’ function was used to fit the coordinates in least square principle. The Binomial curve (syntax:  $y=Ax^2+Bx+C$ ) was shown in Figure 2A. Afterwards, Polynomial curve [syntax:  $p(x)=p_1x^n+p_2x^{n-1}+\dots+p_nx+p_{n+1}$ ] were used for corneal curve fitting by using Curve Fitting Tool in Matlab software, which was an interactive environment presented in the form of a graphical user interface. The Polynomial curve was shown in Figure 2B. After that, Conic section (syntax:  $Ax^2+Bxy+Cy^2+Dx+Ey+F=0$ ) was applied for curve fitting. The conic curve was shown in Figure 2C and the programming codes were shown as follows:

```
xy=[x,y];x=xy(:,1); y=xy(:,2); p=[x.^2, x.*y, y.^2, x, y]\
ones(size(x));
ezplot(@(x,y) p(1)*x.^2+p(2)*x.*y+p(3)*y.^2+p(4)*x+
p(5)*y-1, [0 868 0 380])
```

In order to compare the fitting effects of these three curves, one image among these 15 patients was selected randomly for further analysis. Eight points whose x-coordinates had the fixed interval (100, 200, ...600, 800), which passed the corneal surface equally were selected. Paired *t*-test (Codes:  $[h,p,ci,stats]=ttest2(x,y,0.05,'both')$ ) was used in Matlab to compare the according y-coordinates of each curve equation (yellow arrow in Figure 2) and the simulative incident angles in each selected points between these three curve equations.

Base on theorem of the calculus and trigonometry, the tangent line and normal line at any point in the selected curve equation could be calculated by utilizing ‘diff’ function. Thus, simulative incident angles from a distance could be acquired (red arrow in Figure 2).

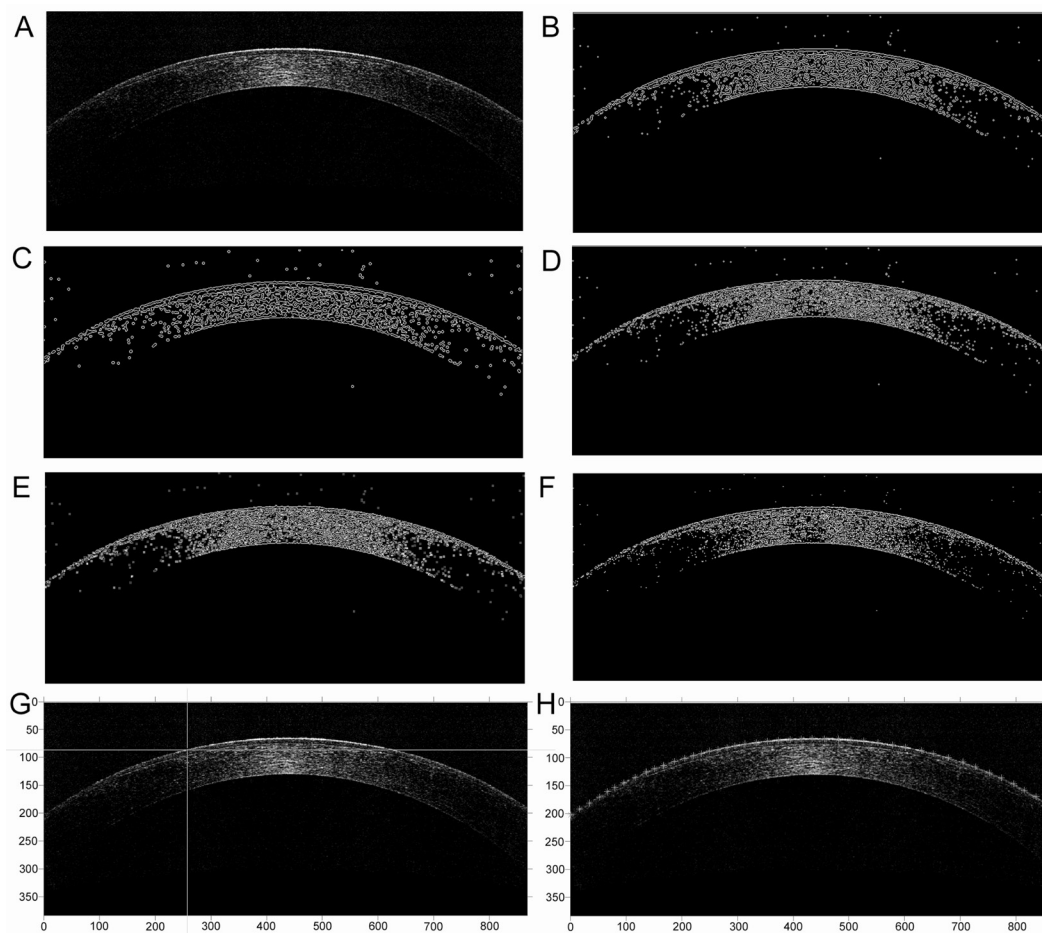


**Figure 1 Corneal surface edge detection** This is one of these images from 15 volunteers. A: Original image; B: Canny edge detection; C: Log edge detection; D: Sobel edge detection; E: Prewitt edge detection; F: Roberts edge detection; G: Manual ginput methods; H: Manual getpts methods.

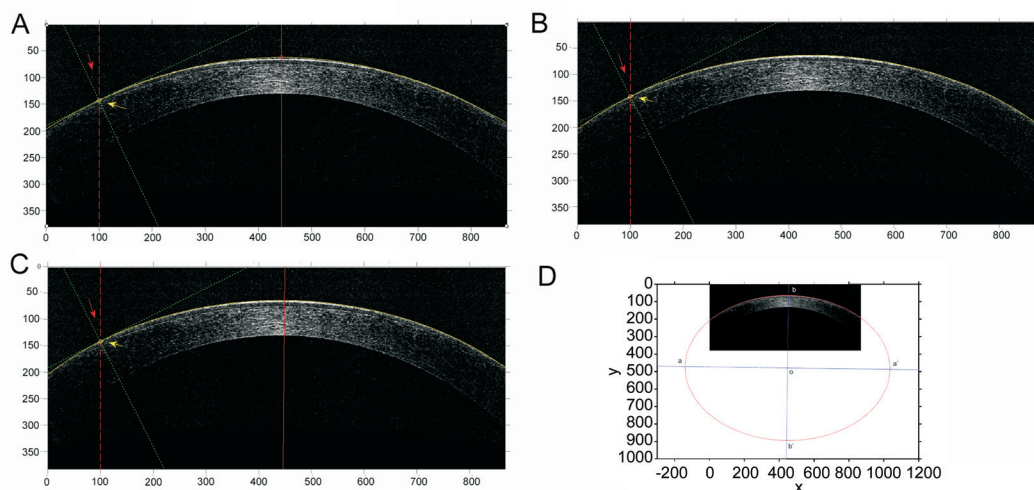


**Figure 2 Comparison between three corneal curve fitting equations** A: Binomial curve (syntax:  $y=Ax^2+Bx+C$ ); B: Polynomial curve [syntax:  $p(x)=p1x^n+p2x^{n-1} + \dots + pnx+pn+1$ ]; C: The Conic section (syntax:  $Ax^2+Bxy+Cy^2+Dx+Ey+F=0$ ); D: The ‘e’ value calculated by ‘a’ axis and ‘b’ axis. Red line: Symmetry axis; Green dash line: Tangent line and normal; Red dash line: The simulative incoming light; Red arrow: Incident angle; Yellow arrow: The calculated coordinate when x-coordinate was 100. Blue line: The axis, ‘o’ was the circle center, aa’ was the ‘a’ axis, bb’ was the ‘b’ axis. In this way, we could get the ‘e’ value ( $e=0.7070$ ).

The formula was:

$K$ : normal line slopes. Incident angle= $90 \pm \arctan(K)$ .

Afterward, images were rotated clockwise 15 degrees. The same approach was implemented to compare the fitting effects of different equations when the images were tilted.

**Comparison of Eccentricity Values Between Corneal Topography and Conic Section** For a conic section equation,  $Ax^2+Bxy+Cy^2+Dx+Ey+F=0$ , the circle center  $(Xc, Yc)$  was  $Xc=(BE-2CD)/(4AC-B^2)$ ;  $Yc=(BD-2AE)/(4AC-B^2)$ . The tilt angle was  $(1/2) \cdot \arctan [B/(A-C)]$ .

Therefore, the semimajor axis (a) and semiminor axis (b) were able to obtainable. The eccentricity could be defined as the ratio of the linear eccentricity (c, which was equal to  $\sqrt{a^2 - b^2}$ ) to the semimajor axis: that was,  $e=c/a$ . In order to validate the feasibility of the 'e' value of conic section, the 'e' values by corneal topography (Oculus, Germany) and conic section were compared with Paired *t*-test in Matlab.

**RESULTS**

**Edge Detection of Corneal Surface** The returned images of 'Roberts' seemed to have the most meticulous outline, while the image of 'Log' had a gross outline. 'Sobel' was similar to 'Prewitt'. After zoomed in (Figure 3A), the points from 'Canny' had the least missing edge segments as well as false edges, which made the edge curve most smooth and connected. Images of Canny edge detection algorithms were shown in Figure 3A. The measuring points from manual identifying were more close to the inside of actual edges (Figure 3B). The Conic curves which calculated by five edge detection algorithms were shown in Figure 3C. On the whole, they all have the ideal curves that indicated the edges of the corneal surface.

**Comparison of Three Corneal Surface Curve Fitting Methods**

Three fitting curves were shown in Figure 2. On the whole, these three curves all fitted the corneal surface well. The Polynomial curves were observed to have a better fitting effect than Binomial curve (Figure 4A). Further observation showed that the corneal curve of Polynomial fitting was one part of one irregular curve. Beyond the selected interval, the graph showed that the polynomial behavior took over and the approximation quickly deteriorated (Figure 4B). Another observable difference was the symmetry axis (red line) of Binomial curve (Figure 2A) was perpendicular to the x-axis, and the Polynomial curve (Figure 2B) had no symmetry axis. In contrast, the Conic curve (Figure 2C) had a tilted symmetry axis, and the tilt angle could be calculated base on principle of conic section, which was equal to  $(1/2)*\arctan [B/(A-C)]$ . Thus, the tilt angle in this selected corneal image was 89.521°. For further analysis, the according y-coordinates in selected x-coordinates and the simulative incident angles of three curve equations were shown in Table 1. No significant differences were found either y-coordinates or simulative incident angles (Paired *t*-test,  $P>0.05$ ).

In Figure 4C-4E, all images were rotated clockwise 15 degrees, the Binomial curves became diverged obviously (Figure 4C). In contrast, the Polynomial and Conic curves both fitted the corneal surface in satisfactory way (Figure 4D, 4E), and the tilt angle of Conic section could be calculated (104.05°. Green arrow in Figure 4E). The according y-coordinates in selected x-coordinates and the simulative incident angles of polynomial and conic curves were shown in Table 2. No significant differences were found either y-coordinates or simulative incident angles (Paired *t*-test,  $P>0.05$ ).

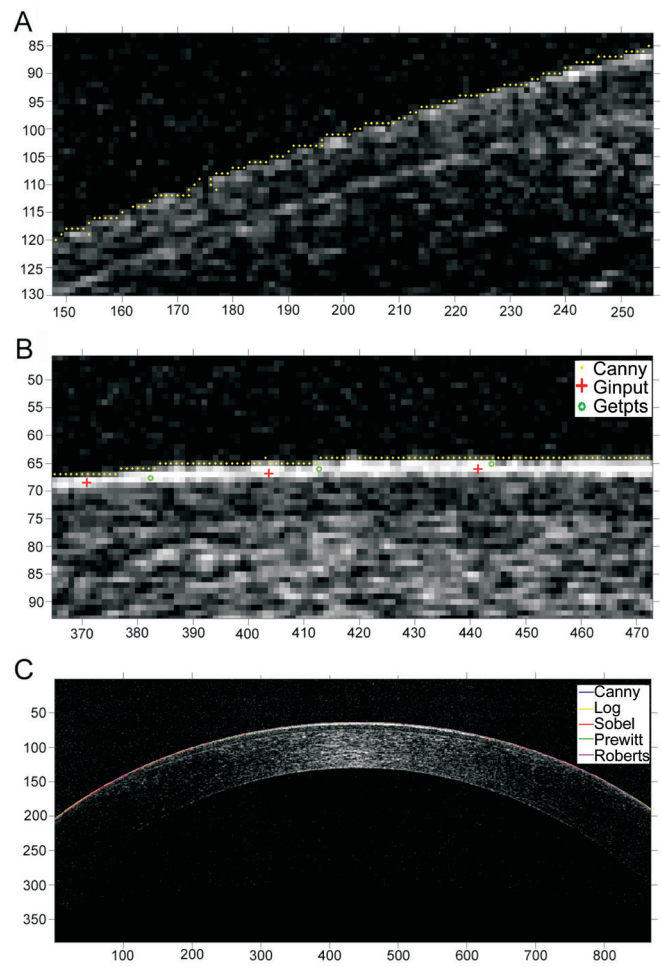


**Figure 3 Comparison between five edge detection methods** Images of Canny edge detection algorithms (A) for fitting curve with conic section. The measuring coordinates of edge detection methods were close to the outside of actual edges. In contrast, measured points of the two manual identifying methods were more close to the inside of actual edges (B). The conic fitting curves between different edges detection methods (C).

**Table 1 The according y-coordinates in selected x-coordinates and the simulative incident angles of three curve equations**

| X-coordinate | Y-coordinate |        |        | Incident angle (°) |        |        |
|--------------|--------------|--------|--------|--------------------|--------|--------|
|              | A            | B      | C      | A                  | B      | C      |
| 100          | 143.10       | 141.44 | 141.34 | 25.258             | 26.691 | 26.640 |
| 200          | 102.82       | 100.87 | 100.79 | 18.483             | 17.716 | 17.698 |
| 300          | 76.25        | 76.14  | 76.23  | 11.131             | 10.132 | 9.999  |
| 400          | 63.45        | 64.76  | 64.96  | 3.390              | 2.870  | 2.903  |
| 500          | 64.40        | 65.92  | 65.94  | 4.476              | 4.157  | 4.019  |
| 600          | 79.11        | 79.31  | 79.21  | 12.178             | 11.105 | 11.139 |
| 700          | 107.56       | 105.71 | 105.93 | 19.459             | 18.579 | 18.895 |
| 800          | 149.77       | 148.20 | 149.06 | 26.143             | 27.913 | 27.959 |

Group A: Binomial curve; Group B: Polynomial curve; Group C: Conic section. Paired *t*-test, y-coordinate: A vs B:  $P=0.34529$ ,  $t=1.0119$ ; A vs C:  $P=0.4757$ ,  $t=0.75355$ ; B vs C:  $P=0.26329$ ,  $t=-1.2163$ . Incident angle: A vs B:  $P=0.68269$ ,  $t=0.42631$ ; A vs C:  $P=0.70093$ ,  $t=0.40022$ ; B vs C:  $P=0.83053$ ,  $t=-0.22216$ .

**Comparison of Eccentricity Values Between Corneal Topography and Conic Section** Eccentricity values measured by corneal topography and calculated by conic section were

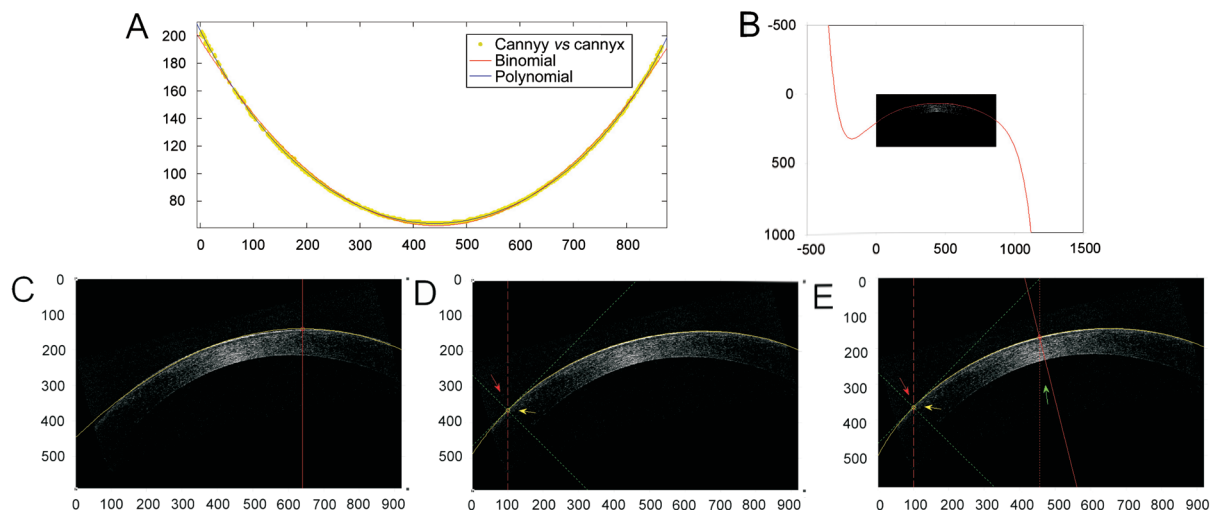


**Figure 4 The curve fitting comparison between three methods** A: The Polynomial curve was found to have a better fitting effect than Binomial curve; B: The graph showed the fitting corneal curve of Polynomial was one part of one irregular curve. Beyond the selected interval the graph showed that the approximation quickly deteriorated; C: The fitting curves when the image was rotated 15 degrees: Binomial curve (syntax:  $y=Ax^2+Bx+C$ ); D: Polynomial curve [syntax:  $p(x)=p_1x^n+p_2x^{n-1} + \dots + p_nx+pn+1$ ]; E: Conic section (syntax:  $Ax^2+Bxy+Cy^2+Dx+Ey+F=0$ ).

**Table 2 The according y-coordinates in selected x-coordinates and the simulative incident angles of polynomial curve and Conic section after the image was rotated 15 degrees**

| X-coordinate | Y-coordinate |        | Incident angle (°) |        |
|--------------|--------------|--------|--------------------|--------|
|              | B            | C      | B                  | C      |
| 100          | 365.12       | 365.02 | 45.172             | 45.532 |
| 200          | 281.51       | 281.53 | 34.616             | 34.466 |
| 300          | 223.49       | 223.67 | 25.751             | 25.741 |
| 400          | 183.35       | 183.49 | 18.059             | 18.095 |
| 500          | 157.56       | 157.61 | 10.869             | 10.919 |
| 600          | 144.68       | 144.65 | 3.787              | 3.808  |
| 700          | 144.37       | 144.39 | 3.508              | 3.595  |
| 800          | 157.55       | 157.69 | 11.738             | 11.701 |

Group B: Polynomial curve; Group C: Conic section. Paired *t*-test, y-coordinate: B vs C:  $P=0.18999$ ,  $t=-1.4513$ . Incident angle: B vs C:  $P=0.4174$ ,  $t=-0.86169$ .

presented in Table 3. No significant differences of ‘e’ value were observed between corneal topography and conic section.

**DISCUSSION**

**Edge Detection of Corneal Surface** In five edge detections, the Canny edge detector is regarded as the state-of-the-art edge detector<sup>[20]</sup>. In the current study, the returned image of Canny was found to have a most smooth and integrated curve. Nevertheless, on the whole, five edge detection algorithms all had the continuous curves which indicated the edges of the corneal surface (Figure 3G). Few differences were found in the final detecting curves. Edge detection technique thereby provided a validated unbiased parameter for rapid and highly reproducible quantification of the level of the corneal curve of the OCT image. Meanwhile, the coordinates from two manual identifying methods were found more close to the

**Table 3 The refractive parameters of fifteen volunteers and comparison of eccentricity values between corneal topography and conic section**

| n  | Age (a) | Refraction (D)     | Corneal curvature | Eccentricity       |               |
|----|---------|--------------------|-------------------|--------------------|---------------|
|    |         |                    |                   | Corneal topography | Conic section |
| 1  | 11      | -4.0Ds             | 42.25             | 0.56               | 0.66          |
| 2  | 10      | -3.5 Ds            | 42.5              | 0.56               | 0.48          |
| 3  | 8       | -2.5 Ds            | 45                | 0.53               | 0.5           |
| 4  | 9       | -2.5 Ds            | 45.25             | 0.62               | 0.65          |
| 5  | 8       | -2.0 Ds-0.5 Dc*170 | 42                | 0.77               | 0.71          |
| 6  | 8       | -2.0 Ds            | 42                | 0.75               | 0.81          |
| 7  | 9       | -1.25 Ds           | 40.5              | 0.57               | 0.5           |
| 8  | 7       | -1.5 Ds            | 41                | 0.57               | 0.61          |
| 9  | 9       | -1.0 Ds            | 40.25             | 0.65               | 0.6           |
| 10 | 10      | -4.75 Ds           | 44.25             | 0.51               | 0.52          |
| 11 | 11      | -4.5 Ds-2.0 Dc*155 | 44                | 0.41               | 0.43          |
| 12 | 11      | -4.75 Ds           | 42.75             | 0.28               | 0.42          |
| 13 | 9       | -5.0 Ds            | 42.5              | 0.45               | 0.52          |
| 14 | 10      | -1.75 Ds           | 41.5              | 0.56               | 0.51          |
| 15 | 11      | -1.25 Ds           | 40.8              | 0.61               | 0.66          |

$t=0.9143$ ,  $P=0.3760$   
(paired *t*-test)

inside of actual edge, which might attribute to position the cursor with the mouse to acquire the coordinates from the corneal surface. Thus, the deviation might increase during this process. Comparatively, the cursor of ‘getpts’ could be visible by operator, and be easier to position corneal surface edge. Because edges extracted from selected images were often hampered by fragmentation, which meaning that the edge curves were not continuous, missing edge segments as well as false edges not corresponding to interesting phenomena

in the image. The manual identifying approach was less affected by definition. Thus, through data merge technology, the deflected points from edge detection could be corrected by manual identifying approach. Thereby, the manual identifying approach was also an essential supplement of edge detection to define the corneal surface edge.

**Comparison of Corneal Surface Curve Fitting** After acquiring the coordinates from the corneal surface, current research selected according y-coordinates and simulative incident angles in selected x-coordinates to compare three fitting curves. Because one important application of such a mathematical model was to study light refraction. In this way, we could turn the comparison to a statistical process (*t*-test). No significant differences were found either y-coordinates or simulative incident angles. Overall they all seemed to be the alternative approaches. Apparently, the Binomial was the most convenient. It used 'polyfit' function to get the equation and required least calculations. Binomial curve has been successfully used in many different fields of optics<sup>[21-23]</sup>. Nevertheless, there are some discussions regarding the applicability and precision when applied to surfaces such as the human cornea: first, Binomial (syntax:  $y = Ax^2 + Bx + C$ , degree  $n=2$ ) was a special case of Polynomial [syntax:  $p(x) = p_1x^n + p_2x^{n-1} + \dots + p_nx + p_{n+1}$ ], the fitting degree of precision was not as good as Polynomial curve (Figure 3A). Secondly, the Binomial curve, namely, parabola was also one kind of Conic curve, and the eccentricity of parabola was always 1. However, the eccentricity from conic curve suggested the corneal curve was an ellipse (Figure 2D,  $0 < e < 1$ ), but not parabola. Finally, Binomial was greatly affected by tilt angle. The symmetry axis of Binomial curve was perpendicular to the x-axis. Therefore, the shortcomings became particularly apparent when the corneal image was tilted (Figure 4C).

Compared with Binomial, the Polynomial curve was able to find the optimal coefficients of a polynomial  $p(x)$  of degree  $n$  that fitted the data best. Thus, Polynomial curve had a comparably more accurate fitting effect in selected interval. Polynomials appear in a wide variety of areas of mathematics, and it is quite suitable in fitting some irregular curves<sup>[24-25]</sup>. However, depending on the algorithm, it is usually best to choose as low a degree as possible for an exact match on all constraints if an approximate fit is acceptable, because there may be a divergent case, where the exact fit cannot be calculated, or it might take too much computer time, it is better to averaging out questionable data points in a sample, rather than distorting the curve to fit them exactly. In Figure 4B, we found Polynomial curve was one irregular curve, beyond the selected interval the graph showed the polynomial behavior took over and the approximation quickly deteriorated. Besides, not all the tilted corneal surface could be fitted by using polynomial curve. Despite the Polynomial curve had

a good fitting effect when the corneal image was slanted 15 degrees (Figure 4D). Obviously, if the image was rotated to a horizontal position, the functional relationship between x and y-coordinates would disappear. So, these imperfections showed Polynomial was also not an ideal corneal surface fitting way.

In the current study, no significant differences between polynomial and conic curve were found either y-coordinates or simulative incident angles (Tables 1, 2). It indicated the conic section also owned a satisfactory fitting effect. In mathematics, a conic section (syntax:  $Ax^2 + Bxy + Cy^2 + Dx + Ey + F = 0$ ) is a curve obtained as the intersection of a cone with a plane. Conic section has certain spherical properties that make them a meaningful expansion set for the description of general arc curve like corneal surfaces in the fields of optical engineering and in physiological optics. This point makes it more advantageous than other available approaches. Compared with the other two curve equations, conic section has a tilted axis of symmetry (when  $B \neq 0$ ). The optical axis of the human eye is coincident with the visual system's mechanical axis, and the axis passes through the center of curvature of each corneal surface, and coincides with the axis of rotational symmetry. Although the rotation of axes requires complex calculations including trigonometry and calculus, this was quite convenient in numerical computing environment like Matlab. In our study, the tilt angle of selected corneal surface image was  $89.521^\circ$ , when the selected image was slanted at a  $15^\circ$  tilt, the calculated tilt angle was  $104.45^\circ$ . Thus, the difference value was  $14.929^\circ$ . This result showed the conic equation had a powerful function to calculate the rotational symmetry of one selected conics.

Base on geometrical principle, a circle has an eccentricity of zero, so the eccentricity shows how 'un-circular' the curve is. Bigger eccentricities are less curved. Traditionally, the three types of conic section are the hyperbola ( $e > 1$ ), the parabola ( $e = 1$ ), and the ellipse ( $0 < e < 1$ ). The circle is a special case of the ellipse ( $e = 0$ ). In our study, the calculated eccentricity also suggested the corneal curve was a changing ellipse. The optical strength of the cornea is much greater than the strength of the eye-lens, and most of the focusing of the lens combination in humans is due to this part of the optical system<sup>[26]</sup>. In this current research, we compared the eccentricity values between corneal topography and conic section. No significant differences of 'e' values were observed between corneal topography and conic section. It also proved the effectiveness of this method with conic curve fitting technology.

The shortcoming of this method was the comparatively complex calculated process, but this method was quite useful especially when the ocular parameters could not be obtained by routine equipment. For example, we could use this method to calculate a much accurate curvature of guinea pigs although the cornea is too much steep and beyond the range of

curvimeter. The current researches focused on the feasibility of edge detection and precision of curve fitting. Next, our further work will use this method to measure eyeball dimensions and some other important parameters like corneal curvature, etc.

In conclusion, our study proved it was feasible to develop mathematical stimulating curve for corneal surface with the help of Matlab software. Edge detection techniques, especially 'Canny' had better repeatability and higher efficiency for corneal surface detection, while the manual identifying approach was also proved to be an indispensable complement. Polynomial and conic section were both the alternative approaches for corneal curve fitting. Overall, conic curve was the optimal choice, because the specific geometrical properties were very advantageous in the research of optical engineering.

### ACKNOWLEDGEMENTS

We would like to thank Prof. Ji-Chang He who reviewed and edited the paper. We would like to thank Jennifer Bruhn for technical assistance in the current research.

**Foundations:** Supported by the National Natural Science Foundation of China (No.81400428); Science and Technology Commission of Shanghai Municipality (No.134119b1600).

**Conflicts of Interest:** Di Y, None; Li MY, None; Qiao T, None; Lu N, None.

### REFERENCES

- 1 Artal P, Herreros DTP, Munoz TC, Green DG. Retinal image quality in the rodent eye. *Vis Neurosci* 1998;15(4):597-605.
- 2 Rosenblum WM, Shealy DL. Computerized analysis of the image quality of the human eye with optical aids. *Am J Optom Physiol Opt* 1975;52(8):561-566.
- 3 Campbell FW, Gubisch RW. Optical quality of the human eye. *J Physiol* 1966;186(3):558-578.
- 4 Bakaraju RC, Ehrmann K, Papas E, Ho A. Finite schematic eye models and their accuracy to in-vivo data. *Vision Res* 2008;48(16):1681-1694.
- 5 Hirano M, Yamasaki K, Okada H, Sakurai T, Kondoh T, Katafuchi T, Sugimura K, Kitazawa S, Kitazawa R, Maeda S, Tamura S. Ray tracing analysis of overlapping objects in refraction contrast imaging. *Radiat Med* 2005; 23:386-389.
- 6 Einighammer J, Oltrup T, Bende T, Jean B. Real ray tracing simulation versus clinical outcomes of corneal excimer laser surface ablations. *J Refract Surg* 2010;26(9):625-637.
- 7 Strom AR, Cortes DE, Rasmussen CA, Thomasy SM, McIntyre K, Lee SF, Kass PH, Mannis MJ, Murphy CJ. In vivo evaluation of the cornea and conjunctiva of the normal laboratory beagle using time- and Fourier-domain optical coherence tomography and ultrasound pachymetry. *Vet Ophthalmol* 2016;19(1):50-56.
- 8 Lai T, Tang S. Cornea characterization using a combined multiphoton microscopy and optical coherence tomography system. *Biomed Opt Express* 2014;5(5):1494-1511.
- 9 Garvie MR, Burkardt J, Morgan J. Simple finite element methods for approximating predator-prey dynamics in two dimensions using MATLAB. *Bull Math Biol* 2015;77(3):548-578.
- 10 O'Connor S, Gaddis R, Anderson E, Camesano TA, Burnham NA. A high throughput MATLAB program for automated force-curve processing using the AdG polymer model. *J Microbiol Methods* 2015;109:31-38.
- 11 Irianto J, Lee DA, Knight MM. Quantification of chromatin condensation level by image processing. *Med Eng Phys* 2014;36(3):412-417.
- 12 Kemeny SF, Clyne AM. A simplified implementation of edge detection in MATLAB is faster and more sensitive than fast fourier transform for actin fiber alignment quantification. *Microsc Microanal* 2011;17(2): 156-166.
- 13 Pedge NI, Walmsley AD. Combining self-modeling curve resolution methods and partial least squares to develop a quantitative reaction monitoring method with minimal reference data. *Appl Spectrosc* 2007; 61(9):940-949.
- 14 Keles H, Naylor A, Clegg F, Sammon C. The application of non-linear curve fitting routines to the analysis of mid-infrared images obtained from single polymeric microparticles. *Analyst* 2014;139(10):2355-2369.
- 15 Yap CH, Thiele K, Wei Q, Santhanakrishnan A, Khiabani R, Cardinale M, Salgo IS, Yoganathan AP. Novel method of measuring valvular regurgitation using three-dimensional nonlinear curve fitting of Doppler signals within the flow convergence zone. *IEEE Trans Ultrason Ferroelectr Freq Control* 2013;60(7):1295-1311.
- 16 Tejedor J, Gutierrez-Carmona FJ. Polynomial curve fitting of the corneal profile in 2.2-mm corneal incision phacoemulsification. *J Refract Surg* 2015;31(1):42-47.
- 17 Deane AS, Kremer EP, Begun DR. New approach to quantifying anatomical curvatures using high-resolution polynomial curve fitting (HR-PCF). *Am J Phys Anthropol* 2005;128(3):630-638.
- 18 Hart J. Mathematics walks into history. *Nature* 2011;476(7359):152.
- 19 Benes P, Synek S, Petrova S. Corneal shape and eccentricity in population. *Coll Antropol* 2013;37(Suppl 1):117-120.
- 20 Sim KS, Tso CP, Ting HY. Canny optimization technique for electron microscope image colourization. *J Microsc* 2008;232(2):313-334.
- 21 Tran P, Waller L. Variability in results from negative binomial models for Lyme disease measured at different spatial scales. *Environ Res* 2015;136:373-380.
- 22 Chiriac A, Foia L, Chiriac AE, Pinteala T, Solovan C, Brzezinski P. Psoriasis and tuberculosis binomial distribution? *J Res Med Sci* 2014; 19(5):477.
- 23 Bandyopadhyay U, Mukherjee S, Dutta D. A randomized test for the conditional odds ratio of matched pairs in an inverse binomial sampling design. *Biom J* 2014;56(6):963-972.
- 24 Helzer A, Barzohar M, Malah D. Stable fitting of 2D curves and 3D surfaces by implicit polynomials. *IEEE Trans Pattern Anal Mach Intell* 2004;26(10):1283-1294.
- 25 Rayces JL. Least-squares fitting of orthogonal polynomials to the wave-aberration function. *Appl Opt* 1992; 31(13):2223-2228.
- 26 Artal P, Berrio E, Guirao A, Piers P. Contribution of the cornea and internal surfaces to the change of ocular aberrations with age. *J Opt Soc Am A Opt Image Sci Vis* 2002;19(1):137-143.